Shengdi Zhang[1] and Hongling Chen[1]

Preparation of Silicone Emulsion Defoamer with Easy Separation of Magnetic Hydrophobic Nanoparticles

To prepare lyophobic magnetic nanoparticles (LMNs) with core/shell structure to be applied in silicone emulsion defoamer, magnetic nanoparticles covered with silica (MNS) were prepared in a one-step process from $FeCl_3 \cdot 6H_2O$, $FeCl_2 \cdot 4H_2O$ and tetraethyl orthosilicate and then modified with poly (methylhydrosiloxane). X-ray powder diffraction (XRD), scanning electron microscope (SEM), Fourier transform infrared spectroscope (FTIR), thermogravimetric analysis (TGA), and contact angle tests were performed to characterize the nanoparticles, and the droplets of the defoamer emulsion were observed with a microscope. The foam breaking and foam inhibition properties of the defoamer and the magnetic separation of the particles were observed and recorded by a camera. It was found that the silicone emulsion defoamer exhibited good foam breaking and foam inhibition properties for foaming systems with anionic, cationic and non-ionic surfactants, respectively. The solid particles in the defoamer could be easily separated from the defoamed systems by a magnet.

Key words: Magnetic nanoparticles, Defoaming agent, Antifoaming agent, Emulsion separation, Hydrophobic modification

Herstellung eines Silikonemulsions-Entschäumers mit einfacher Abtrennung von magnetischen hydrophoben Nanopartikeln. Zur Herstellung lyophober magnetischer Nanopartikel (LMNs) mit Kern-Schale-Struktur, die in Silikon-Emulsionsentschäumern angewendet werden sollen, wurden magnetische Nanopartikel, die mit Siliziumdioxid (MNS) beschichtet sind, in einem einstufigen Prozess aus $FeCl_3 \cdot 6H_2O$, $FeCl_2 \cdot 4H_2O$ und Tetraethylorthosilikat hergestellt und anschließend mit Poly(methylhydrosiloxan) modifiziert. Zur Charakterisierung der Nanopartikel wurden Messungen mit der Röntgenpulverbeugung (XRD), dem Rasterelektronenmikroskop (SEM), dem Fourier-Transform-Infrarot-Spektroskop (FTIR), die thermogravimetrische Analyse (TGA) sowie Kontaktwinkeltests durchgeführt, wobei die Tröpfchen der Entschäumeremulsion mit dem Mikroskop beobachtet wurden. Die schaumbrechenden und schauminhibierenden Eigenschaften des Entschäumers sowie die Magnetabscheidung der Partikel wurden mit der Kamera beobachtet und aufgezeichnet. Es zeigte sich, dass der Silikonemulsions-Entschäumer gute schaumbrechende und schauminhibierende Eigenschaften für schäumende Systeme mit anionischen, kationischen bzw. nicht-ionischen Tensiden aufweist. Die Feststoffpartikel im Entschäumer konnten leicht mit einem Magneten von den entschäumten Systemen getrennt werden.

[1] College of Chemical Engineering, Nanjing Tech University, Nanjing 211816, P.R. China.

Stichwörter: Magnetische Nanopartikel, Entschäumer, Emulsionstrennung, hydrophobe Modifikation

1 Introduction

Undesirable foam is sometimes a major problem in industrial production [1–3]. A defoamer is regarded as the most effective, economical, and convenient way to eliminate foam [4, 5]. Commonly used types of defoamer in industry include alcohols, phosphates esters, fatty acids, and silicones, etc. [6, 7]. Defoamers should possess two functions: defoaming and antifoaming, i. e. the abilities of foam breaking and foam inhibition. Among the various types of defoamers, silicone emulsion defoamer with oil phase, which is composed of poly(dimethylsiloxane) (PDMS) and hydrophobic particles, is widely used in detergent industry [8], food industry [9] and medical field [10], etc.

Denkov has studied the defoaming process of silicone emulsion defoamers with hydrophobic silica and described the importance of hydrophobic particles as the essential active component for defoaming to reduce the "barrier to entry" [11]. The defoaming mechanism of silicone emulsion defoamer is shown in Fig. 1. The defoamer is immersed in the film of foam as oil droplets in which the hydrophobic particles are dispersed. The hydrophobic particles keep the droplets stable while reducing the "entry barrier" of the oil droplets by destabilizing the asymmetric oil-water-air films ("pin effect") (Fig. 1a).

Meanwhile, the oil droplets carry particles through the Plato boundary between the foams and penetrate the foam film to form an oil bridge (Fig. 1b). The bridge is stretched until a thin oil film forms in the center of the bridge. The entire foam film is destroyed by the rupture of the oil film and the dewetting of the hydrophobic particles (Fig. 1c).

Based on the above mechanism, the hydrophobic particles play an important role in the defoaming process. However, these particles would not be separated but dispersed in the solution after the end of defoaming process. In most cases, these hydrophobic particles, which are usually lyophobic modified silica, would not be seriously harmful, but in some fields such as food industry, fermentation industry or pharmaceutical production, etc., the residues of these foreign particles are unacceptable.

The traditional hydrophobic particles are small in size and quantity, and there is no report about the separation of hydrophobic particles from the system after defoaming. Herein we designed a defoamer with lyophobic magnetic nanoparticles (LMNs). The LMNs were designed as a core-shell

structure with the magnetic material as the core, which enables direct separation with a magnet, and the silica coating as the shell, which is further lyophobically modified. Liu et al. [12] modified Fe_3O_4@SiO_2 by growing ZIF-8 to obtain a hydrophobic magnetic adsorbent with a high specific surface area, which could efficiently adsorb bisphenol A and be rapidly separated by a magnet. Qu et al. [13] hydrophobized Fe_3O_4@SiO_2 particles with octyl trimethoxy silane to form a Pickering emulsion, and immobilized the enzyme on the surface of the particles. Enzyme-loaded particles were used as the catalyst for the esterification of 1-hexanol and hexanoic acid, and were separated easily with a magnet after reaction. However, no attention has been paid to the defoamer with magnetic hydrophobic nanoparticles for separation.

In this study, we prepared magnetic nanoparticles covered with silica (MNS) as the precursor by a one-step process and modified MNS with polymethylhydrosiloxane (PMHS) to obtain LMNs for the preparation of silicone emulsion defoamer. MNS and LMNs were characterized, and the defoaming and antifoaming abilities of the prepared defoamer and the separability of the particles were tested as well.

2 Experimental

2.1 Materials

Tetraethyl orthosilicate, $FeCl_3 \cdot 6H_2O$, $FeCl_2 \cdot 4H_2O$, cyclohexane, Twen80, Span80, dodecyl trimethyl ammonium bromide, ammonia solution (25%) and sodium dodecyl benzene sulfonate were purchased from Shanghai Lingfeng Chemical Reagent Co., Ltd., China. Anhydrous ethanol was purchased from Wuxi City Yasheng Chemical Co., Ltd., China. Poly(dimethylsiloxane) (PDMS, viscosity values: 350 mPa · s and 500 mPa · s at 25 °C) and polymethylhydrosiloxane(PMHS, hydrogen content: 1.56%) were kindly supplied by Dow Corning(Shanghai) Co., Ltd., China. Hydroxyethyl cellulose was obtained from Nanjing Profem chemical (Jiangsu) Co., Ltd., China. Lutensol A3N and Lutensol A9N were obtained from BASF-Ypc Co., Ltd. The Anti Sudsing Agent LN1414 was obtained from Advanced Chemical Co., Ltd. Distilled water was used in all experiments. All the chemicals were used without further purification.

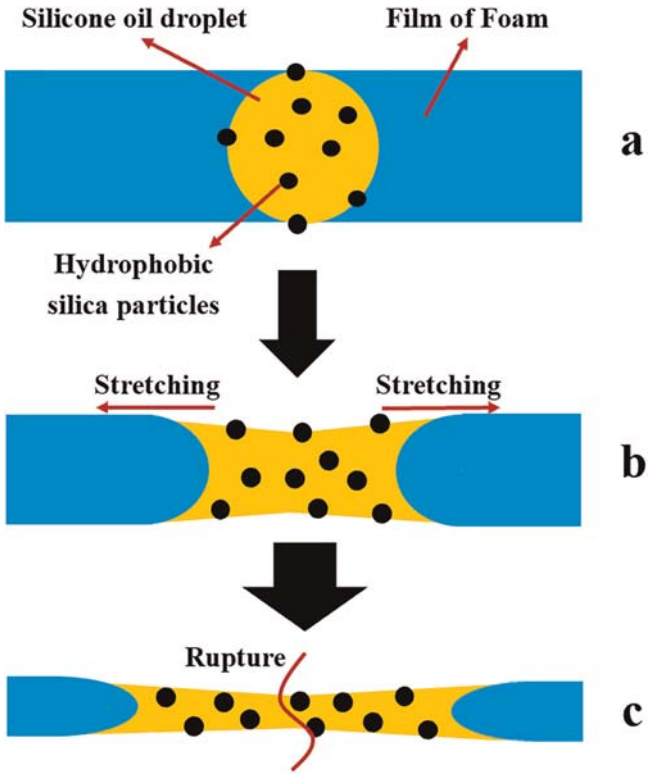

Figure 1 The steps of silicone emulsion in defoamer breaking the foam film: (a) Forming oil bridge with the "pin effect" of hydrophobic silica particles. (b) The "bridging-stretching" effect. (c) The rupture of foam film

2.2 Preparation of MNS

The one-step process which is combination of the co-precipitation method (synthesis of Fe_3O_4) and the Stober method (coating of SiO_2) was used to prepare MNS [14]. 3.65 g $FeCl_3 \cdot 6H_2O$ and 1.35 g $FeCl_2 \cdot 4H_2O$ were dissolved in 60 ml water. The resulting solution was stirred for 10 min at 60 °C in nitrogen atmosphere. After that 6 ml ammonia solution was added, and the mixture was stirred for 2 h to form a suspension with small magnetic core particles. Then 60 ml ethanol and 4 ml tetraethyl orthosilicate were added to the suspension and stirred for 4 h to coat the magnetic paticles with silica. Afterwards, the particles were separated by magnets, washed with ethanol and water for three times, and dried in vacuum oven for 12 h at 60 °C to obtain MNS.

2.3 Preparation of LMNs

First, 1 g of the prepared MNS was dispersed in 30 g of cyclohexane by ultrasonication, then 1 g of PMHS was added as a modifier and stirred for 30 min at 25 °C. After the modification, the particles were separated by magnets, washed three times with cyclohexane and ethanol, and dried in vacuum oven for 6 h at 60 °C to obtain LMNs.

2.4 Preparation of silicone emulsion defoamer

0.35 g LMNs and 10 g PDMS (a mixture of 5 g PDMS with a viscosity of 350 mPa · s and 5 g PDMS with a viscosity of 500 mPa · s) were mixed, heated to 180 °C, and stirred for 2 h to obtain compound A. The mixture was then mixed with the emulsifier. The prepared compound A was mixed with 2.5 g of emulsifier containing 29.1% Twen80, 21.9% Span80 and 50% Lutensol A3N (AEO-3), and with 30 g of 1 wt% aqueous hydroxyethylcellulose solution, then heated to 50 °C and stirred at high speed for 30 min to obtain the silicone emulsion defoamer.

2.5 Characterizations

The crystal forms of MNS were characterized by an X-ray powder diffraction (XRD, Bruker D8 Advance) with Cu-Kα radiation. The morphology of MNS and LMNs were observed by a scanning electron microscope (SEM, Carl Zeiss AG GeminiSEM 300) at 5 kV acceleration voltage. The static contact angles of particles were measured by an automatic contact angle detector (Solon Tech SL200B), after the sample

was pressed in a tablet (Shanghai Shengli SL252). The functional groups of particles were analyzed by Fourier transform infrared spectrometry (FT-IR, Rayleigh WQF-510A). The thermal stabilities of particles were determined by a thermogravimetric analyzer (TGA, DTG-60H Shimadzu) at a heating rate of 10 °C/min from 20 °C to 800 °C under air atmosphere. The silicone emulsion defoamer was observed by an optical microscope GaleIV-3 from Cambridge Instruments.

2.6 Tests of defoaming and antifoaming abilities

The defoaming and antifoaming abilities of defoamer were tested in the foaming solution of sodium dodecyl benzene sulfonate (SDBS), dodecyl trimethyl ammonium bromide (DTAB) and Lutensol A9N (AEO-9), which represent anionic, cationic, and non-ionic surfactants, respectively. The Bartsch method [15] was chosen to measure the defoaming and antifoaming abilities: 10 mL of 0.5 wt% foaming solution was added to a 100 ml measuring cylinder with stopper, and the cylinder was shaken for 30 s at a frequency of 3 times/s to generate foam. The volume of original foam was recorded as V_0. Then ca. 50 mg of defoamer was added to the measuring cylinder, and the volume of foam after 30 s of defoaming was recorded as V_1. Afterwards, the foam solution with defoamer was shaken for 30 s at the same frequency, and the volume of foam after antifoaming was recorded as V_2. Finally, we calculated the defoaming efficiency and the antifoaming property:

$$\eta_1 = \frac{V_0 - V_1}{V_0} \times 100\ \% \quad (1)$$

$$\eta_2 = \frac{V_0 - V_2}{V_0} \times 100\ \% \quad (2)$$

where η_1 is the defoaming efficiency, η_2 is the antifoaming efficiency. Furthermore, the defoaming and antifoaming properties of the blank emulsion (silicone emulsion without LMNs) and the commercial defoamer Anti Sudsing Agent LN1414 were also tested under the same conditions. All the experiments were repeated three times, and the average and standard deviation of the results were calculated.

3 Results and discussion

3.1 Crystal forms of MNS

The XRD pattern of MNS was shown in Fig. 2. The diffraction peaks at $2\theta = 30^\circ$, 35.44°, 43.24°, 53.54°, 57.22° and 63.06° were indexed to the crystal planes of 220, 311, 400, 422, 511 and 440 respectively, which was consistent with the standard spectra of Fe_3O_4 or γ-Fe_2O_3, indicating that the composition of the core was Fe_3O_4 or γ-Fe_2O_3, or both [16, 17]. The small peak near $2\theta = 18.22^\circ$ was due to the existence of amorphous silica.

3.2 Morphology of MNS and LMNs

SEM images of MNS and LMNs were shown in Fig. 3. It can be seen from the images that both MNS and LMN are monodisperse particle aggregates with a particle size of about 40 nm, and hydrophobic modification with PMHS hardly changed the particle size and dispersion state.

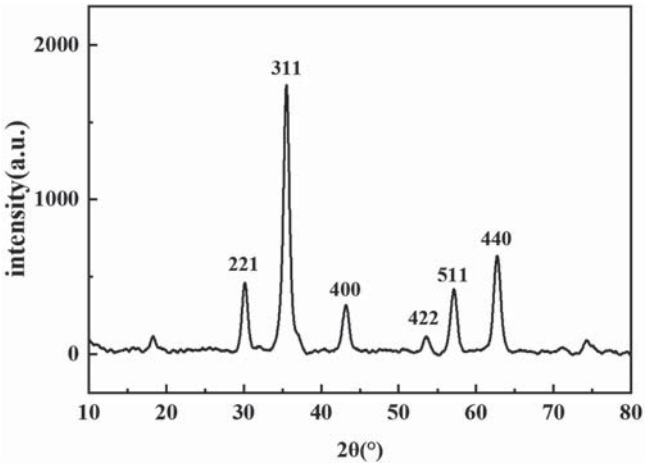

Figure 2 The XRD pattern of MNS

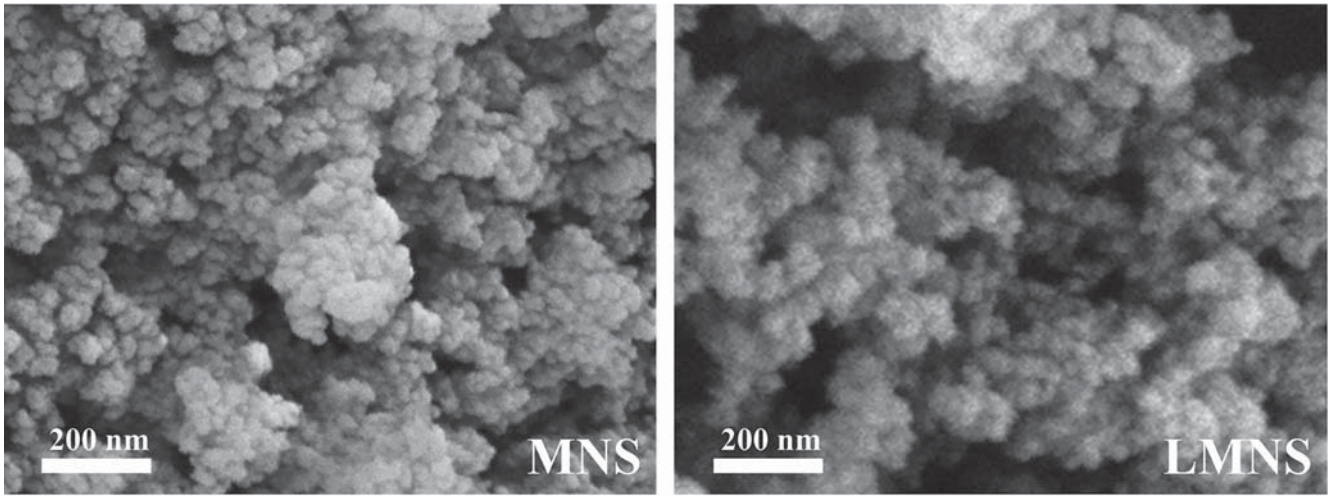

Figure 3 The SEM images of MNS and LMNs

3.3 Contact angles of MNS and LMNs

Ca. 10 mg sample powder was pressed into thin slice by SL252 tablet press. Then the thin slice was put on the platform of SL200B automatic contact angle detector, and 10 μL water was dropped onto the surface of the thin slice. The picture and data of the contact angle were recorded. As shown in Fig. 4, the contact angle of the particle increased from almost 0° to 142° after the modification of PMHS, indicating that the particles changed from hydrophilic to strongly hydrophobic, which met the requirements of defoamer.

3.4 FTIR determination of MNS and LMNs

The FTIR spectra of MNS and LMNs were shown in Fig. 5. Both MNS and LMNs had broad peaks near 3414 cm^{-1}, 1641 cm^{-1} and 1100 cm^{-1}, which corresponded to the stretching vibration of –OH group, the bending vibration of H–O–H bond and the symmetric stretching of Si–O–Si bond, respectively. These were the characteristic peaks of SiO_2. Compared to MNS, additional peaks at 2928 cm^{-1} and 2858 cm^{-1} were detected in the spectrum of LMN, which corresponded to the tensile vibration of the $–CH_3$ and $–CH_2$ groups introduced by PMHS, while the peaks observed at 1411 cm^{-1} and 2167 cm^{-1} are due to the bending vibration of the Si–C group and the stretching vibration of the Si–H group in the PMHS structure, respectively [18]. All these bands indicated that PMHS was grafted onto the surface of SiO_2 shell.

3.5 Thermal stability of MNS and LMNs

The TGA curves of the MNS and LMNs in the air atmosphere are displayed in Fig. 6. The weight loss of the two types of particles below 120 °C was mainly due to the loss of free water adsorbed on the surface. The loss of free water of LMNs was obviously less than that of MNS because of the hydrophobic modification. The weight loss of MNS in the range of 120 °C to 800 °C was caused by the dehydrogenation of silicon hydroxyl on the surface of silica shell. For LMNs, the weight loss between 120 °C and 800 °C was associated with the thermal decomposition of surface-grafted PMHS chains and dehydration of the remaining silicon hydroxyl. Above 450 °C the weight loss of LMNs was essentially the same as that of MNS, indicating that the thermal decomposition of surface-grafted PMHS was essentially complete at 450 °C.

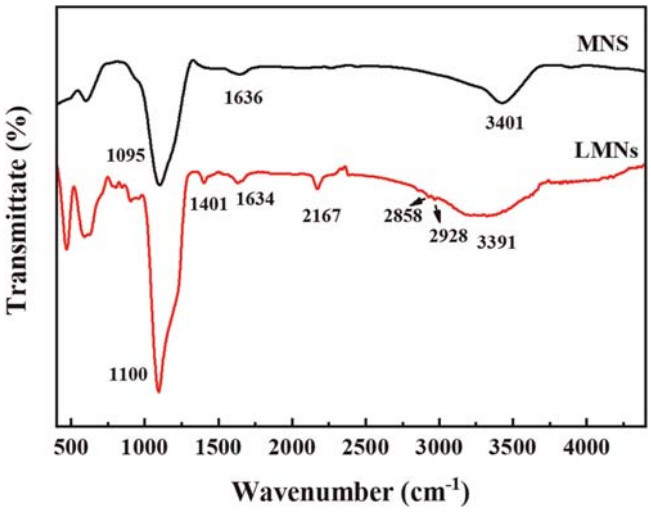

Figure 5 The FTIR spectra of MNS and LMNs. Conditions of measurement: The sample powder was mixed with KBr, and the mixture was pressed at 10 MPa for 30 s. The range of wavenumber was 450 cm^{-1}–4 500 cm^{-1}

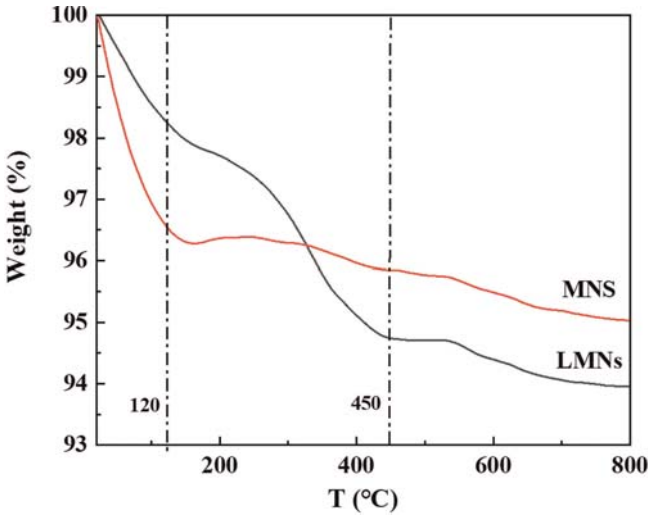

Figure 6 The TGA curves of MNS and LMNs,Conditions of measurement: Air atmosphere. The rate heating was 10 °C/min. The range of temperature was 25 °C–800 °C

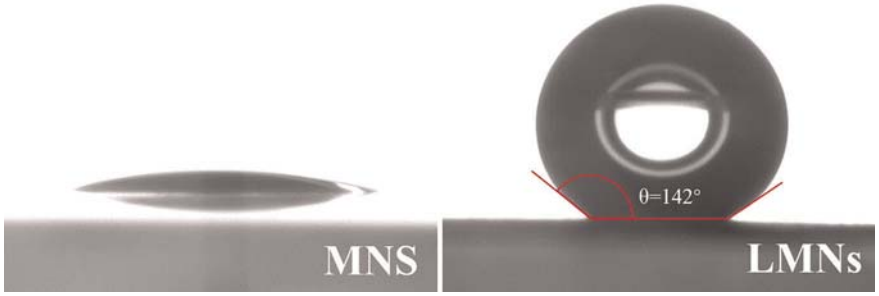

Figure 4 The static contact angles of MNS and LMNs. Conditions of measurement: The sample powder were pressed at 10 MPa for 30 s. The thin slice was placed on a glass slide, and 10 μm water was dropped on the surface of sample under the room temperature

3.6 Characterization and tests of silicone emulsion defoamer

The suspension was sampled and observed with a light microscope. The photos in Fig. 7a show that the prepared silicone suspension is uniform and has the brownish-red color of γ-Fe_2O_3. In the microscopic image, droplets containing brownish-red LMNs particles are clearly visible in the emulsion. The size distribution of the droplets was calculated with software and the result is shown in Fig. 7b. The average size of the emulsion droplets was (10.19 ± 5.08) μm.

As the photos in Fig. 7c–7e show, that the foam generated in the solutions as described in Section 2. 6 was eliminated after the addition of the defoamer, and the regeneration power of the foam was greatly reduced. After defoaming, no colored oil spots were observed on the wall, which means that all particles were suspended in the liquid.

The results of the defoaming and anti-foaming experiments are shown in Fig. 8. Solutions of 0.5 wt% each of SDBS and DTAB and AEO-9, respectively, were prepared and foamed. The defoamer prepared with LMN was added to these surfactant solutions. It was found that the defoamer prepared with LMN has both defoaming and anti-foaming properties. Within 30 s, a defoaming efficiency of 100% was achieved for all three surfactant solutions. The antifoaming efficiency was also more than 90% with the silicone defoamer with LMN. In comparison, the defoaming and antifoaming properties of the silicone oil emulsion without LMNs (blank sample) were significantly worse than those of the defoamer with LMNs for all surfactant solutions studied, indicating the important role of hydrophobic magnetic nano particles for the defoamer. The commercial defoamer LN1414 had good defoaming and anti-foaming properties in the SDBS solution and the AEO-9 solution, but its defoaming ability was not satisfactory in the DTAB solution. The obtained results show that the defoamer with LMN particles prepared in this work seems to have better defoaming and defoaming performance with SDBS, DTAB and AOE-9 surfactant solutions compared to the commercial defoamer LN1414. However, the situation could be completely different if tested with a different foaming solution, since a defoamer is a specialty chemical whose action is specifically tailored to its application. Therefore, different defoamers have their own suitable applications, and it is difficult to say which one is better.

We also found that the antifoaming ability of the defoamer in the foaming solution of SDBS was generally lower than that in the DTAB and AEO-9 solutions, which might be because the nature and structure of the foaming surfactant can influence the antifoaming effect. The charges on the hydrophilic head of the anionic surfactant SDBS ensured that both sides of the foam film had the same charge, so the repulsion of the charges can protect the foam film from thinning. The defoamer had the strongest defoaming effect in the foaming solution that contained the nonionic surfactant AEO-9, because the foam produced by AEO-9 was the least with its low-

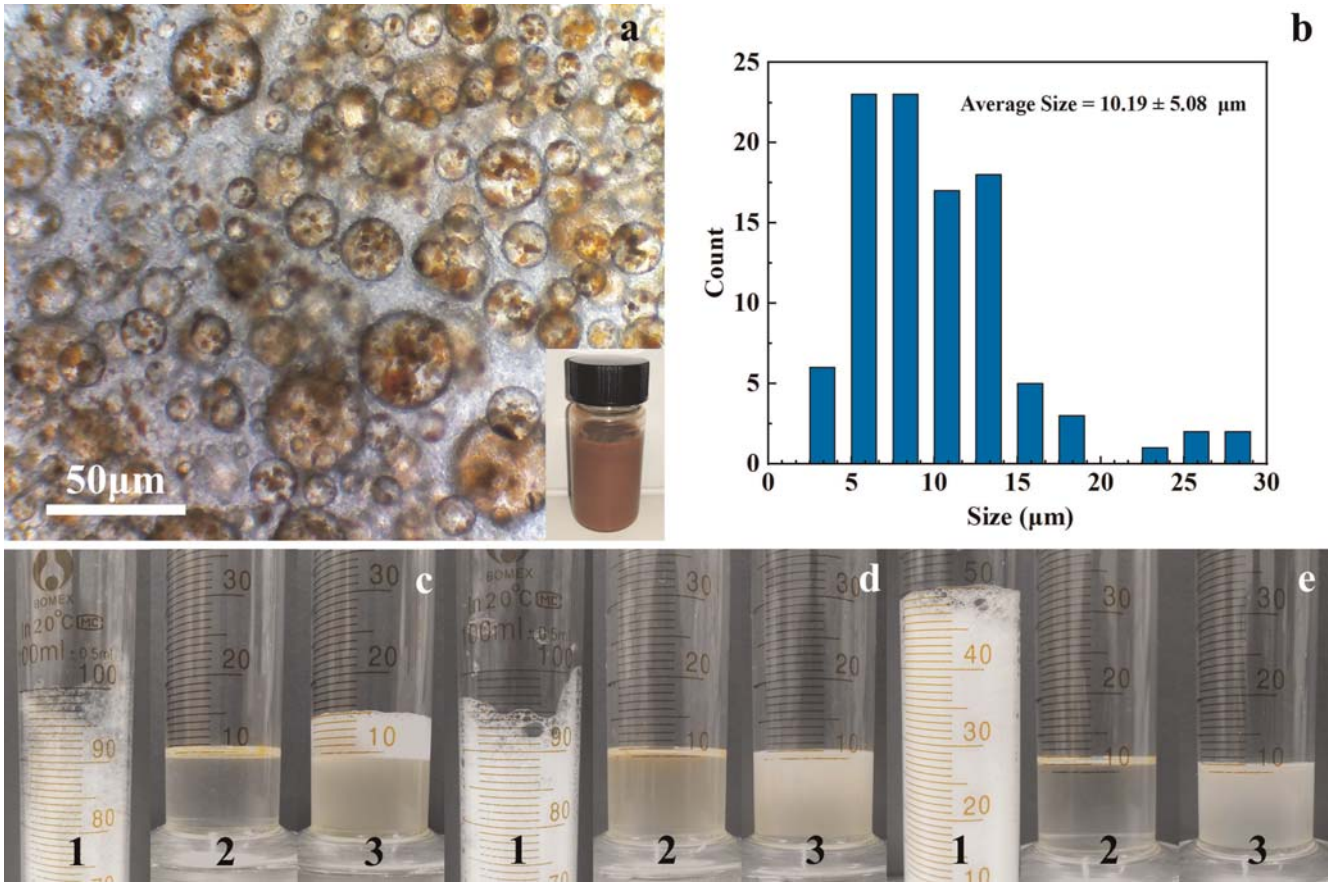

Figure 7 (a) The photograph and optical micrograph of the silicone emulsion. (b) The distribution of defoamer emulsion's droplet size. The photos of (1) original foam, results of (2) defoaming experiment and (3) antifoaming experiments in 0.5 wt% (c) SDBS, (d) DTAB and (e) AEO-9 as foaming solution

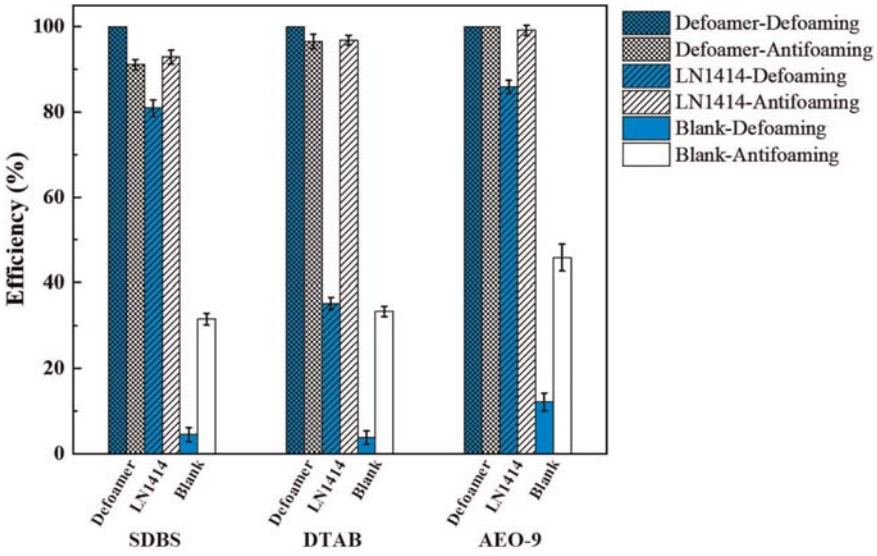

Figure 8 The defoaming and antifoaming efficiencies of the defoamer with LMNs, the blank emulsion without LMNs and Anti Sudsing Agent LN1414 in 0.5 wt% SDBS, DTAB and AEO-9 solution

er charge repulsion. Comparing SDBS with CTAB, the hydrophilic end of SDBS is not as branched as that of DTAB. When the surfactant molecules were arranged at the interface of the foam film, the molecules of SDBS showed a more compact state, so that the foam film could restore the foam state more quickly. For CTAB, the absorption layer of surfactant molecules on the liquid film was not so compact due to branching. Therefore, the defoamer showed a better antifoam effect in the foam produced by DTAB. But in general, the defoamer had good defoaming and anti-foaming efficiency for all foams generated with the three surfactant types.

To investigate the effect of acid or alkali on the defoaming and antifoaming effect of the defoamer, the pH value of foaming solution was adjusted from 2 to 12 by HCl or NaOH.

From Fig. 9a, it can be seen that the defoaming effect of the defoamer in the foaming solution of the three surfactants changed little in the pH range from 2 to 12. From Fig. 9b, it can be seen that the defoaming effect of the defoamer in the foam solution of the three surfactants became lower when the pH was lower than 4, and that it also became lower in the foam solution of the two ionic surfactants SDBS and DTAB when the pH increased up to 8.

Although the silica layer was modified by PMHS, a residue of unmodified –OH remained, which determined the surface charge properties of the particles. The zero charge point of silica is pH 2.5, so when the pH was close to 2, the charges of the particles became zero and the repulsion became weaker, which was not conducive to the diffusion of the particles and was unfavorable to the antifoam effect of the particles. When the pH was greater than 8, there were more negative charges on the particle surfaces, which caused the particles to approach (for surface activity of the cationic surfactants) or repel (for surface activity of the anionic surfactant) the hydrophilic head of the surfactants, which was not conducive to the occurrence of antifoaming at the interface. For the newly added particles, defoaming occurred in a short time, and the effect of acid or alkali on the surface charge property of the particles was not obvious, so it had little effect on the defoaming effect.

As the photos in Fig. 10 show, the added defoamer was dispersed in the foaming solutions of the three surfactants

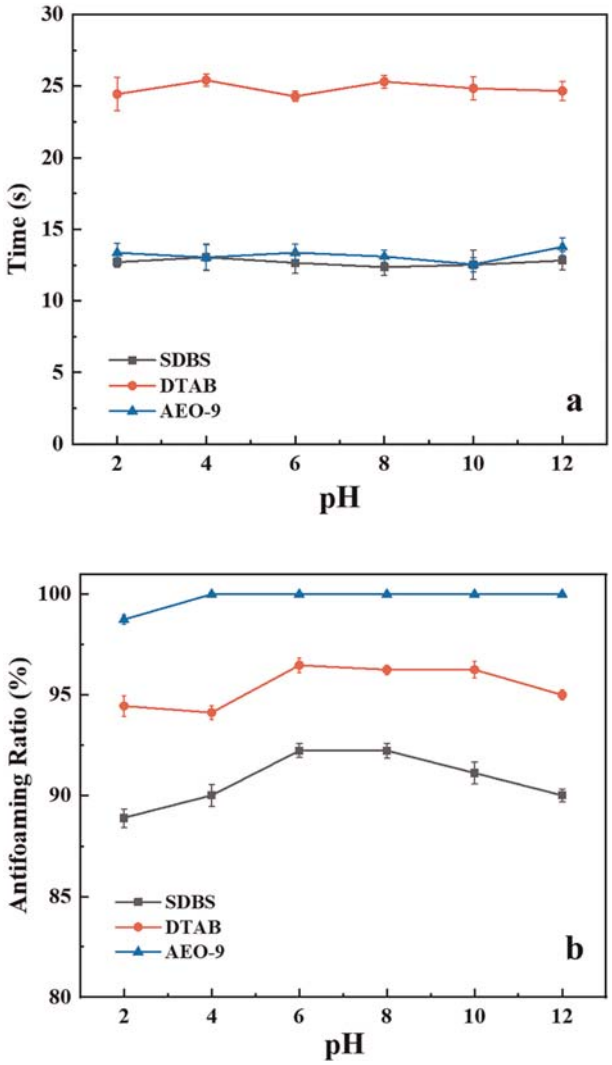

Figure 9 (a) The defoaming time and (b) the antifoaming efficiency of defoamer in foaming solutions with different pH of defoamer in foaming solutions with different pH

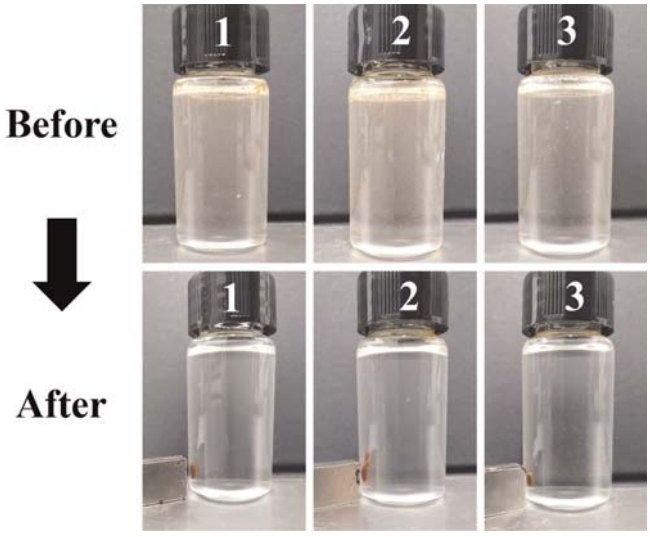

Figure 10 The magnetic separation of the defoamer particles from the 0.5 wt % (1) SDBS (2) DTAB (3) AEO-9 foaming solution

and the suspensions were all uniform. By applying an external magnetic field, the magnetic particles of the defoamer collected in the direction of the magnet and were easily separated from the foaming solution.

4 Conclusions

In conclusion, core-shell magnetic hydrophobic particles, LMNs, were prepared and applied in a silicone emulsion defoamer. The defoamer showed good defoaming and antifoaming efficiency in foaming systems of different surfactants, even in the acidic or alkaline environment. All the hydrophobic particles in defoamer could be directly separated by magnet, which can effectively reduce the residue or contamination in the foaming solution.

Acknowledgements

This work is financially supported by Nanjing Green Interface New Materials Research Institute Co., Ltd. and Jiangsu Sixin Scientific-Technological Application Research Institute Co., Ltd.

References

1. *Moeller, L.* and *Görsch, K.*: Foam formation in full-scale biogas plants processing biogenic waste. Energy, Sustainability and Society, *5, 1* (2015) 1 – 16. DOI:10.1186/s13705-014-0031-7
2. *He, Q., Li, L., Zhao, X., Qu, L., Wu, D.* and *Peng, X.*: Investigation of foaming causes in three mesophilic food waste digesters: reactor performance and microbial analysis. Scientific Reports, 7, *1* (2017) 1 – 10. DOI:10.1038/s41598-017-14258-3
3. *Gurevich, A. E., Endres, B. L., Robertson, J. O.* and *Chilingar, G. V.*: Gas migration from oil and gas fields and associated hazards. Journal of Petroleum Science and Engineering, *9, 3* (1993) 223 – 238. DOI:10.1016/0920-4105(93)90016-8
4. *Nielsen, J. C., Felipe, S. D. O. L., Rasmussen, T. G., Thykr, J., Workman, C. T.* and *Basso, T. O.*: Industrial antifoam agents impair ethanol fermentation and induce stress responses in yeast cells. Applied Microbiology and Biotechnology, *101, 22* (2017) 8237 – 8248. DOI:10.1007/s00253-017-8548-2
5. *Galgoci, E. C., Chan, S. Y.* and *Yacoub, K.*: Innovative, Gemini-type molecular defoamer technology for improved coating aesthetics. Jct Research, *3, 1* (2006) 77 – 85. DOI:10.1007/s11998-006-0008-3
6. *Liu, Y.* and *Zhu, Z.*: Alkyl Alcohols as Defoamers to Remove Foam Generated by Partially Alcoholyzed Polyvinyl Alcohol for Warp Sizing. AATCC Journal of Research, *6, 4* (2019) 3. DOI:10.14504/ajr.6.4.3
7. *Kougias, P. G., Boe, K.* and *Angelidaki, I.*: Solutions for foaming problems in biogas reactors using natural oils or fatty acids as defoamers. Energy & Fuels, *29, 7* (2015) 4046 – 4051. DOI:10.1021/ef502808p
8. *Sawicki, G. C.*: Impact of surfactant composition and surfactant structure on foam control performance. Colloids and Surfaces A: Physicochemical and Engineering Aspects, *263, 1* (2005) 226 – 232. DOI:10.1016/j.colsurfa.2004.12.026
9. *Pelton, R.* and *Flaherty, T.*: Defoamers: Linking fundamentals formulations. Polymer International, *52*, *4* (2003) 479 – 485. DOI:10.1002/pi.1203
10. *Birtley, R. D. N., Burton, J. S., Kellett, D. N., Oswald, B. J.* and *Pennington, J. C.*: The effect of free silica on the mucosal protective and antiflatulent properties of polydimethylsiloxane. The Journal of pharmacy and pharmacology, *25, 11* (1973) 859 – 63. DOI:10.1111/j.2042-7158.1973.tb09963.x
11. *Denkov, N. D., Marinova, K. G.* and *Tcholakova, S. S.*: Mechanistic understanding of the modes of action of foam control agents. Advances in Colloid & Interface Science, *206* (2014) 57 – 67. DOI:10.1016/j.cis.2013.08.004
12. *Liu, J. F., Qiu, H. J., Zhang, F.* and *Li, Y.*: Zeolitic imidazolate framework-8 coated Fe_3O_4@SiO_2 composites for magnetic solid-phase extraction of bisphenols. New Journal of Chemistry, *44, 14* (2020) 5324 – 5332. DOI:10.1039/D0NJ00006J
13. *Qu, Y.,Huang, R.,Wei, Q.,Qi, Q.* and *He, Z.*: Structural Insight into Stabilization of Pickering Emulsions with Fe_3O_4@SiO_2 Nanoparticles for Enzyme Catalysis in Organic Media. Particle & Particle Systems Characterization, *34, 7* (2017) 1700117. DOI:10.1002/ppsc.201700117
14. *Chen, J. J.* and *Chen, H. L.*: Removal of anionic dyes from an aqueous solution by a magnetic cationic adsorbent modified with DMDAAC. New Journal of Chemistry, *42, 9* (2018) 7262 – 7271. DOI:10.1039/C8NJ00635 K
15. *Denkov, N. D.*: Mechanisms of foam destruction by oil-based antifoams. Langmuir, *20, 22* (2004) 9463 – 9505. DOI:10.1021/la049676o
16. *Stjerndahl, M., Andersson, M., Hall, H. E., Pajerowski, D. M., Meisel, M. W.* and *Duran, R. S.*: Superparamagnetic Fe_3O_4/SiO_2nanocomposites: enabling the tuning of both the iron oxide load and the size of the nanoparticles. Langmuir, *24, 7* (2008) 3532 – 3536. DOI:10.1021/la7035604
17. *Sun, Y., Duan, L., Guo, Z., Duanmu, Y., Ma, M., Xu, L., Zhang, Y.* and *Gu, N.*: An improved way to prepare superparamagnetic magnetite-silica core-shell nanoparticles for possible biological application. Journal of Magnetism & Magnetic Materials, *285*(1 – 2) (2005) 65 – 70. DOI:10.1016/j.jmmm.2004.07.016
18. *Zhang, Y., Chen, H., Wen, Y., Yuan, Y., Wu, W.* and *Liu, C.*: Tunable wettability of monodisperse core-shell nano-SiO_2 modified with poly(methylhydrosiloxane) and allyl-poly(ethylene glycol). Colloids & Surfaces A: Physicochemical & Engineering Aspects, *441* (2014) 16 – 24. DOI:10.1016/j.colsurfa.2013.08.079

Received: 20.09.2020
Accepted: 27.12.2020

Bibliography
DOI 10.1515/tsd-2020-2312
Tenside Surf. Det. 58 (2021) 2, page 114 – 120

ISSN 0932-3414 · e-ISSN 2195-8564

Correspondence address

Dr. Hongling Chen
College of Chemical Engineering
Nanjing Tech University
Nanjing 211816
P.R. China
Fax: +86 25 83587206
E-Mail: hlchen@njtech.edu.cn

The authors of this paper

Dr. Hongling Chen (Ph. D), a professor of the College of Chemical Engineering in Nanjing Tech University of China, obtained his bachelor and master degrees in East China University of Science and Technology and completed his Ph. D studies from Nanjing Tech University. Currently, he is mainly engaged in the research and teaching in the fields of fine and specialty chemicals. He has published the book "Introduction to Fine Chemicals". He also has published more than 100 papers in domestic and international journals, and has authorized more than ten invention patents.

Shengdi Zhang, a postgraduate student in College of Chemical Engineering, Nanjing Tech University (China). His graduation dissertation is focused on the application of magnetic materials with surficial modification in chemical processes.